

## Thermomechanical Modeling of an Exhaust Manifold

Intan K Kushairi<sup>1</sup>, Mokhtar Awang<sup>1\*</sup>, Aidil Ab Rahman<sup>1</sup>, Ichsan S Putra<sup>2</sup>, Iman Kartolaksiono<sup>2</sup>

<sup>1</sup>Institute of Transport Infrastructure, Universiti Teknologi PETRONAS, 32610 Seri Iskandar, Perak, Malaysia

<sup>2</sup>National Center for Sustainable Transportation Technology, CRCS Building, 2nd Floor, Institut Teknologi Bandung, Indonesia

\*Email: [mokhtar\\_awang@utp.edu.my](mailto:mokhtar_awang@utp.edu.my)

### Abstract

The commonly used form of transportation mostly relies on-road vehicles nowadays. A vehicle is a mechanism to commute between places with higher efficiency and less time consumption. A vehicle usually consists of multiple working components, in which the engine is well-known to be one of its most crucial components. Although it can be considered the most vital component in a vehicle, the knowledge gaps for an engine are still unlimited. So much more potential can be explored for an engine to reach its maximum capabilities. Part of the perspective that should be explored is to study the engine's thermal properties. This paper aims to investigate the effect of varying temperatures at the exhaust manifold under a certain amount of time spans. The temperature varied from low to high and vice versa for 6 cycles. The results revealed that the exhaust manifold had undergone an alteration in the strain of the body's elasticity. Because of that, the displacement of the exhaust manifold, load distribution, and direction have also been affected.

### Keywords

*Thermomechanical; Modeling; Exhaust manifold; Engine*

## 1 Introduction

The exhaust manifold plays an important role in the combustion engine system. A cylinder head is connected to the exhaust manifold. Hot air from the combustion result is extracted into the exhaust manifold to be purged or returned to the air intake valve using the turbocharger. The exhaust manifold can run almost red hot [1], and sometimes the temperature can increase until 1000 °C when the engine runs hard [2]. When the excessive temperature has reached its point, it will lead to chemical changes in the material. Other than that, the expansion and reaction of the manifold's stress and strain would occur when it is constrained by bolt joints [2]. In real practice, the engine would undergo a low temperature (room temperature) and high temperature (operating temperature), so the stress cycle is developed [3]. It is because the non-linear material's physical properties have been changed during the heating, which causes thermal stress [4]. Such behavior can lead to a more severe condition, fatigue, which needs to be prevented and optimized in the design [5]. Hence, understanding the thermal behavior of the structure for the cyclic temperature is important because the thermal load has a close relationship with low-cycle fatigue phenomena [6].

In this paper, the focus is to see the effect of temperature changing from low to high and vice versa for 6 cycles.

The manifold is restrained from moving by the bolt load. The manifold material uses one of the cast iron materials, with the stress and strain results being the main outcome to be studied.

## 2 Methodology

### 2.1 Geometrical Model

The model used is a V6, four cylinders diesel engine. Figure 1 shows the full model of the engine. The main components are the cylinder head, gasket, bolt, and manifold. Meanwhile, other components are the flame face, engine oil, coolant, and air intake. The meshing of the model was done in Hypermesh. All the components are initially merged to become one single model, which allows sharing of surfaces between the components, and the meshing is done afterward. The meshed model was then exported and imported back into Simlab software. The simulation was done in Simlab because it has a simpler GUI and is more user-friendly.

The analysis consists of two main steps: Thermal Analysis and Thermal Stress Analysis [7]. In Thermal Analysis, initially, the model is running in CFD, which the model has fluid and solid parts, as shown in Figure 2. In the CFD, the model meshed with the existence of a boundary layer, as shown in Figure 3, and underwent a steady state condition. The results from the steady state

became the initial boundary condition for the transient CFD analysis. The transient analysis is vital to provide thermal boundary conditions [8] in which the solid part has non-linear mechanical properties. For the transient case, the model ran under 6 cycles for 0.2 seconds of engine running. Next, the result from the last time steps of transient CFD is taken as an input in structural analysis. Those results are temperature and pressure, which are automatically mapped into the structural case to get stress-strain results.

The thermal stress analysis consists of three important steps [7]. Firstly, the bolt is fastened to the manifold at room temperature. Next, the model is applied to the temperature load from the CFD transient result. Then, the model is cooled to the room temperature again. These three cycles are repeated twice to form six load cases. The cyclic loading is repeated to get the result of stress and strain.

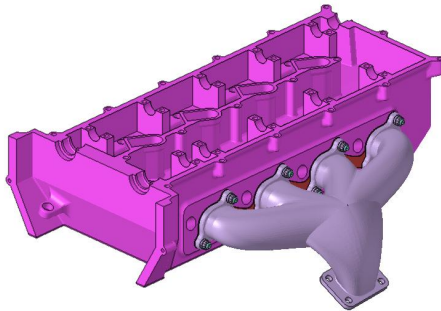


Figure 1 Full model

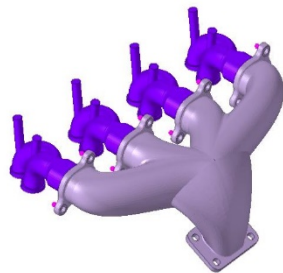


Figure 2 Fluid and solid parts

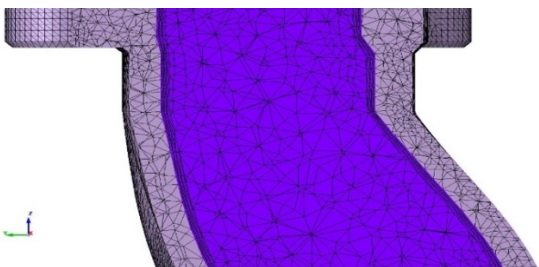


Figure 3 Boundary layers between solid and fluid parts for thermal analysis

## 2.2 Material Properties

The density of the exhaust manifold and the cylinder head is  $7100 \text{ kg/m}^3$  and  $7150 \text{ kg/m}^3$ , respectively. The fluid region uses default air properties. Tables 1 and 2 show the material properties of an exhaust manifold and the other powertrain components.

Table 1 Mechanical properties of exhaust manifold

Temperature (K)	Young's Modulus (MPa)	Poisson's Ratio	Alpha $\cdot 10^{-6}$ (1/K)	Conductivity (W/mK)
293.1	169,000	0.275	11.0	35.50
373.1	167,000	0.275	11.5	35.50
473.1	163,000	0.275	12.0	35.35
293.1	161,000	0.275	12.5	35.20
373.1	158,000	0.275	13.0	35.05
473.1	145,715	0.275	13.1	35.90
293.1	137,563	0.275	14.1	35.75
373.1	125,335	0.275	14.4	35.50

Table 2 Mechanical properties of the other power train components

Parts	Temperature (K)	Young's Modulus (MPa)	Poisson's Ratio	Alpha $\cdot 10^{-6}$ (1/K)	Conductivity (W/mK)
Head	293.1	169,000	0.275	11.0	35.50
Bolts	373.1	167,000	0.275	11.5	35.50
Gasket	473.1	163,000	0.275	12.0	35.35

<sup>a</sup> Cylinder Head.

## 2.3 Boundary Conditions

Figure 4 shows the boundary conditions of the fluid consist of inflow, outflow, and wall type. The inflow of the fluid consisting of temperature and mass flux. The example temperature graph can be seen in Figure 5 below. All the temperature and mass flux values have been input as the Piecewise Linear type, and these values were then multiplied by 750 K and 0.1 kg/s, respectively. The outflow value is constant, 250,000 Pa.

### 2.3.1 Thermal Analysis

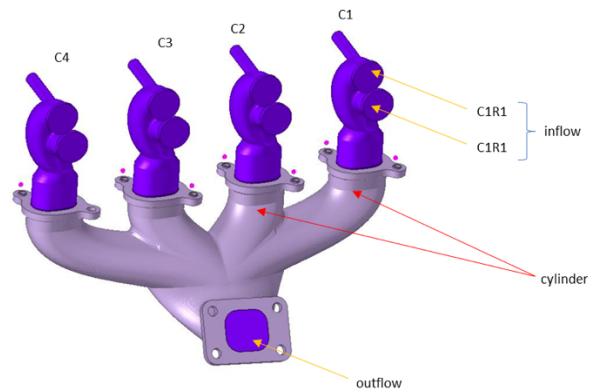


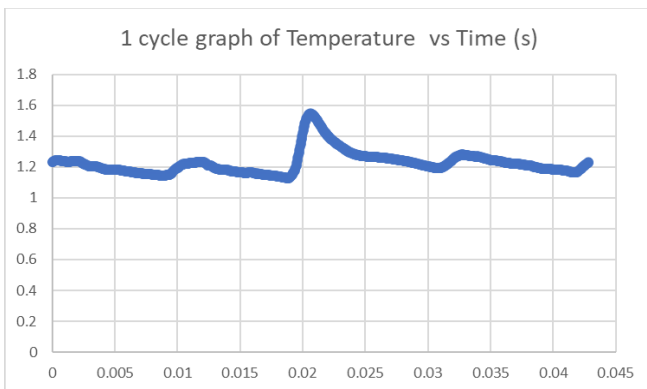
Figure 4 Boundary condition of the fluid

Table 3 shows the boundary conditions for the components. All the components have a convection wall type of heat transfer. However, only the boundary condition of flux wall type with  $0 \text{ W/m}^2 \cdot \text{K}$  is applied on

the sharing surface of the fluid and solid structure, which is the exhaust fluid wall.

**Table 3** Boundary conditions of the wall components

Components	Wall Type	Heat Transfer Coefficient (W/m <sup>2</sup> .K)	Reference Temperature (K)
Flame Face	Convection	657	1000
Manifold	Convection	0.0003	293.15
Engine Oil	Convection	1000	393
Coolant	Convection	9943	363
Air Intake	Convection	125	336
Others	Convection	0	300



**Figure 5** Fluid complete temperature cycle in operating conditions

### 2.3.2 Thermal Stress Analysis

For thermal stress analysis, there are two main boundary conditions. Firstly, the contact between the components. Secondly, the load. There are two types of loads, which are pretension load and thermal load.

The contact preparation is important to see the effect of bolt loading [5]. The contact interfaces are listed below:

- Cylinder head and gasket
- Gasket and manifold
- Manifold and bolt head
- Bolt surfaces and cylinder head
- Bolt surfaces and manifold
- Bolt head and bolt surface

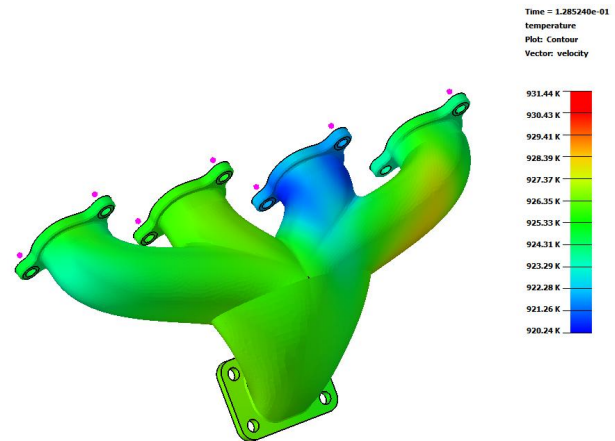
The pretension load is applied to observe the forces acting on the manifold before and after the thermal load is applied. The pretension load is applied initially at room temperature, known as a Cold Case, while the Hot Case is when the thermal load is applied. Both hot and cold cases were running in cyclic cycles to obtain the result of stress and strain on the manifold [9].

## 3 Results and Discussion

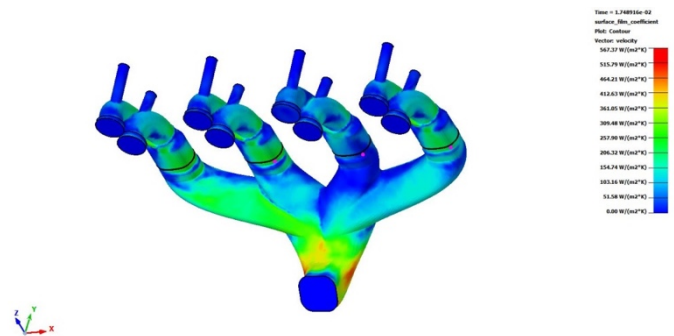
### 3.1 Thermal Analysis Result

Figure 6 shows the temperature distribution of an exhaust manifold at 0.2 sec time step. The maximum

temperature is 931.44 K, and since the running is in a very short period, the C3 temperature is still not fully transferred to the manifold component. Figure 7 shows the Surface Film Coefficient (SFC) result at the end of the time step. This SFC result represents there are heat transfer occurred between the fluid and solid interaction during the simulation [10]. The SFC of the fluid-structural interaction reached a maximum value of 567.37 W/m<sup>2</sup>K.



**Figure 6** Temperature distribution on an exhaust manifold at the end of the transient timesteps



**Figure 7** SFC distribution on the exhaust fluid at the end of the transient timesteps

### 3.2 Thermal Stress Analysis Result

The effect of varying cyclic temperatures would result in changes in the strain of the body's elasticity. There are two strain types of an elastic body, primarily when the component is generated by free expansion; otherwise, the component is generated by internal constraints of various fractions during the thermal analysis [11]. When varying the temperature from cold to hot, the bolt forces also vary [5]. Figure 8 illustrates the manifold bolt behavior during the cyclic loading, Load Case 1 represents a cold situation. Load Case 2 represents hot conditions, and the sequence is repeated thrice. The result from the cyclic loadings is represented in terms of stress variation, as shown in Figure 8.

The displacement of the exhaust manifold is shown in Figure 9. The displacement observed is in the direction

away from the bolt load location. The manifold is stretching away, and the maximum displacement that occurred is 2.59 mm.

The stress distribution during the first Cold Case, where only pretension load is applied, is shown in Figure 10. Figure 11 shows the stress distribution at the end of the last six cycles, where the cold, hot, and cold cases are repeated twice.

The maximum von Mises stress on the manifold during the pretension loading only under the room temperature for Load Case 1 is 36 MPa. The highest temperature occurred in the manifold area, which shared the surface with the bolt. It shows that stress occurs when the pretension load is applied without the temperature existence [9].

When the temperature load is applied to the model, more contoured stresses occur. The stresses emerged bigger on the manifold-bolt area and around the necking of the cylinders. The maximum von Mises stress observed after the whole cyclic loading of room temperature + pretension bolt and operating temperature + pretension bolt on the last cycle is 323 MPa.

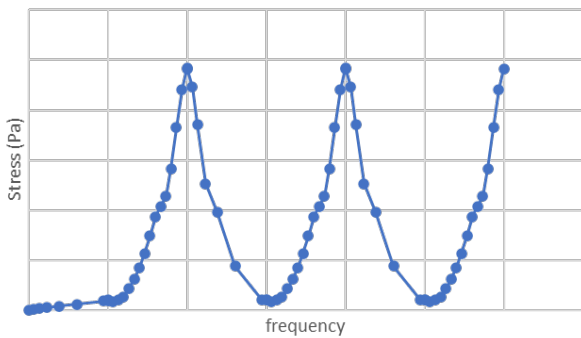


Figure 8 Force variation for manifold loads

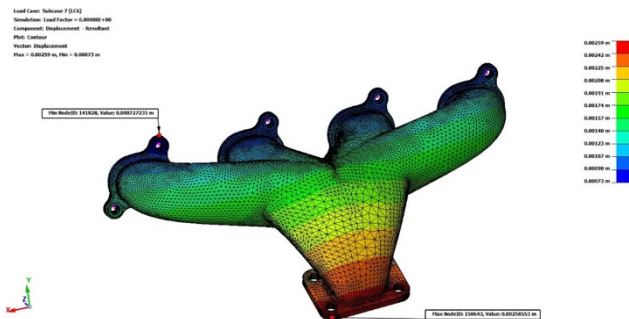


Figure 9 Displacement contour of exhaust manifold

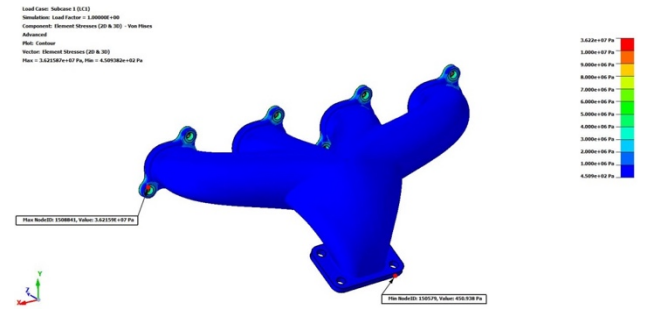


Figure 10 Stress distribution when only pretension are applied under room temperature condition

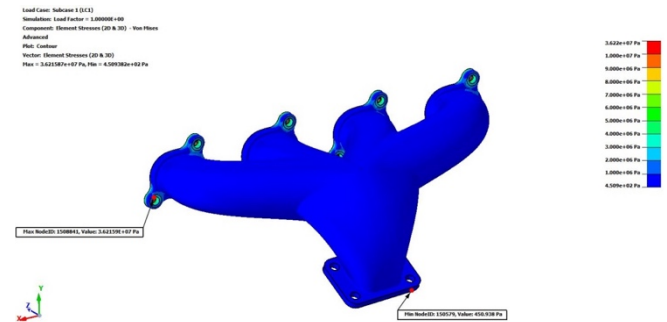


Figure 11 Stress distribution after thermal load are applied at the end of the cyclic loadings

Figure 12 shows the area where plasticity occurred. The equivalent strain occurred on the manifold where the bolt head is located [5] and on the sharp corners between the cylinders.

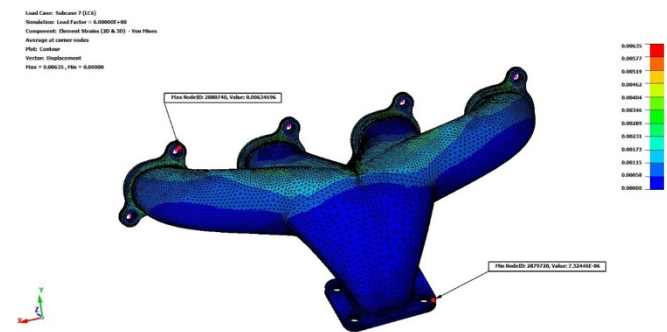


Figure 12 Equivalent plastic strain distribution on exhaust manifold

#### 4 Conclusion

In conclusion, the strain of the body's elasticity has undergone some changes. Consequently, the exhaust manifold displacement and direction had to change to move away from the bolt load location [5]. Furthermore, when the cyclic temperature loading is applied in the simulation, a higher load is expected due to local cyclic plastic straining of the material [2], and higher contoured stresses occur in the figure depicted. The stresses appear higher on the manifold-bolt area and around the necking of the cylinders.

## Acknowledgment

The authors offer their profound thanks to Universiti Teknologi PETRONAS for providing financial aid under an International Collaborative Research Fund, 015ME0-279.

## References

- [1] S. G. Rautrao and B. R. Shinde, "Numerical Study of Exhaust Manifold using Conjugate Heat Transfer," *Int. J. Eng. Adv. Technol.*, no. 5, pp. 2249–8958, 2017.
- [2] T. Gomez and U. Deuster, "Designing Exhaust Manifolds Using Integral Engineering Solutions," *Retrieved*, vol. 1, no. 29, p. 2015, 2009.
- [3] J. C. Crown, "Supersonic nozzle design," no. 2, 1950, [Online]. Available: <http://hdl.handle.net/2060/19930082268>
- [4] B. Zou, Y. Hu, Z. Liu, F. Yan, and C. Wang, "The impact of temperature effect on exhaust manifold thermal modal analysis," *Res. J. Appl. Sci. Eng. Technol.*, vol. 6, no. 15, pp. 2824–2829, 2013, doi: 10.19026/rjaset.6.3792.
- [5] A. De Azevedo Cardoso and E. C. Andreatta, "Thermomechanical Analysis of Diesel Engine Exhaust Manifold," *SAE Tech. Pap.*, vol. Part F1270, no. October, 2016, doi: 10.4271/2016-36-0258.
- [6] S. Sissa, M. Giacopini, and R. Rosi, "Low-cycle thermal fatigue and high-cycle vibration fatigue life estimation of a diesel engine exhaust manifold," *Procedia Eng.*, vol. 74, pp. 105–112, 2014, doi: 10.1016/j.proeng.2014.06.233.
- [7] S. Yoon, K. O. Lee, S. B. Lee, and K. H. Park, "Thermal stress and fatigue analysis of exhaust manifold," *Key Eng. Mater.*, vol. 261–263, no. II, pp. 1203–1208, 2004, doi: 10.4028/www.scientific.net/kem.261-263.1203
- [8] M. Chen, Y. Wang, W. Wu, and J. Xin, "Design of the Exhaust Manifold of a Turbo Charged Gasoline Engine Based on a Transient Thermal Mechanical Analysis Approach," *SAE Int. J. Engines*, vol. 8, no. 1, pp. 75–81, 2014, doi: 10.4271/2014-01-2882.
- [9] S. Patil, S. Biradar, and S. N. Kurbet, "Stress Pattern Analysis in Intake Manifold," pp. 11339–11346, 2017, doi: 10.15680/IJRSET.2017.0606223.
- [10] C. Delprete and C. Rosso, "Exhaust manifold thermo-structural simulation methodology," *SAE Tech. Pap.*, no. 724, 2005, doi: 10.4271/2005-01-1076.
- [11] Z. Yan, L. Zhien, X. Wang, H. Zheng, and Y. Xu, "Cracking Failure Analysis and Optimization on Exhaust Manifold of Engine with CFD-FEA Coupling," *SAE Int. J. Passeng. Cars - Mech. Syst.*, vol. 7, no. 2, pp. 873–881, 2014, doi: 10.4271/2014-01-1710.